GEOPHYSICAL RESEARCH LETTERS, VOL. 37, L01203, doi:10.1029/2009GL041427, 2010

The spectrum of a Saturn ring spoke from Cassini/VIMS

E. D'Aversa,[1] G. Bellucci,[1] P. D. Nicholson,[2] M. M. Hedman,[2] R. H. Brown,[3]
M. R. Showalter,[4] F. Altieri,[1] F. G. Carrozzo,[1] G. Filacchione,[5] and F. Tosi[1]

Received 26 October 2009; revised 30 October 2009; accepted 10 December 2009; published 14 January 2010.

[1] On 2008, July, the Cassini/VIMS spectrometer detected spokes on the Saturn's B ring for the first time. These are the first measurements of the complete reflectance spectrum of the spokes in a wide spectral range (0.35–0.51 μm). Here we will focus on a single broad-shaped spoke, imaged by VIMS on July, 9. Radiative transfer modeling supports a pure water ice composition for the spoke's grains, but their size distribution is found to be wider than previously thought: preliminary results yields a modal value of about 1.90 μm (reff = 3.5 μm, veff = 0.3) and a number density of about 0.01–0.1 grains/cm^3. The unexpected abundance of micron-sized grains in the spoke may have implications for the formation models since the energy requirement increases by at least one order of magnitude. These kind of observations may also constrain the size selection effects thought to be produced by the forces governing the spokes' evolution. **Citation:** D'Aversa, E., G. Bellucci, P. D. Nicholson, M. M. Hedman, R. H. Brown, M. R. Showalter, F. Altieri, F. G. Carrozzo, G. Filacchione, and F. Tosi (2010), The spectrum of a Saturn ring spoke from Cassini/VIMS, *Geophys. Res. Lett.*, *37*, L01203, doi:10.1029/2009GL041427.

1. Introduction

[2] Spokes on the Saturn's rings appear as broad or elongated markings, usually across the outer part of the B ring, not far from the synchronous orbit radius. They are known to form near Saturn's equinoxes, on time scales of the order of minutes and to fade away in a few hours. A lot of physical modeling has been developed about their nature and evolution, but the process of their formation is not yet fully understood and still debated [e.g., *Farmer and Goldreich*, 2005; *Morfill and Thomas*, 2005; *Jones et al.*, 2006]. They have been discovered by Voyager in 1980–81 [*Smith et al.*, 1982], then repeatedly detected in a long-term HST campaign [*McGhee et al.*, 2005], and finally re-observed by the Cassini ISS camera from September 2005 [*Mitchell et al.*, 2006]. All these observations have been obtained using a limited range of spectral filters in the 0.2–1.1 μm spectral range. Here we report about the first observations of spokes at wavelengths longward of 1.1 μm, obtained with the Visual and Infrared Mapping Spectrometer (VIMS) on board the Cassini spacecraft. The spectra, ranging from 0.35 to 5.1 μm and acquired since July 2008, cover the main water ice absorption bands, making these observation very useful in constraining the spoke grains microphysics.

[1]Istituto di Fisica dello Spazio Interplanetario, INAF, Rome, Italy.
[2]Astronomy Department, Cornell University, Ithaca, New York, USA.
[3]Lunar and Planetary Laboratory, University of Arizona, Tucson, Arizona, USA.
[4]SETI Institute, Mountain View, California, USA.
[5]Istituto di Fisica Spaziale e Fisica Cosmica, INAF, Rome, Italy.

0094-8276/10/2009GL041427$05.00

2. VIMS Instrument and Data Reduction

[3] VIMS is an imaging spectrometer covering the 0.35–5.1 μm spectral range in 352 spectral channels. It is able to produce 64 $\times$ 64 pixels images with two distinct channels (VIMS-V, 0.35–1.05 μm, and VIMS-IR, 0.85–5.1 μm). We refer to the paper of *Brown et al.* [2004] for an exhaustive description of the main instrumental issues. Each VIMS spectrum has been accurately georeferenced, by means of specific NAIF-SPICE [*Acton*, 1996] based algorithms, and calibrated following the standard pipeline [*McCord et al.*, 2004] with the latest available upgrades (2009). The main source of measurement errors for the VIMS spectra of the rings is the spatial resolution, which makes the size of the pixels' footprints of the same scale length as the variation of the radiative field.

3. Spoke Observations

[4] Although several spokes have by now been identified in the VIMS data, in the present work we will focus on a single spoke observation, acquired on 2008, July 9th (cube 1594203306). Here a broad spoke appears darker than the surrounding lit face of the B ring by less than 10% (Figure 1). The scene is illuminated 6° over the ring plane, and viewed from 24° elevation with a spatial resolution of about 390 km/pixel in the radial direction and 940 km/pixel in the azimuthal one. Phase angle is 24.5°. Polar projection and azimuthal normalization of the resolved ringlets have been used in order to enhance the shape of the spoke (Figure 1c). It appears roughly elliptical, about 6000 $\times$ 2000 km in size, and tilted by about 70° with respect to the radial direction. It is not spatially homogeneous and its densest part lies very near its outer edge, less than 4000 km from the synchronous radius (SystemIII reference frame). Azimuthally, it is located 18° (30 min) away from the morning Saturn's shadow. Because of the spectral variations among ringlets intrinsic to the B ring structure, the spoke spectra can be meaningfully interpreted only if compared with ring spectra exactly on the same ringlets. The sets of spectra inside the spoke and outside (*reference* spectra) have been defined very carefully, within the actual spatial resolution of the data, in order to avoid the interpretation of the usual variability of the underlying ringlets' structure as a spectral spoke peculiarity (Figure 1c). Further image processing has been applied in order to remove a wavelength-dependent azimuthal trend of

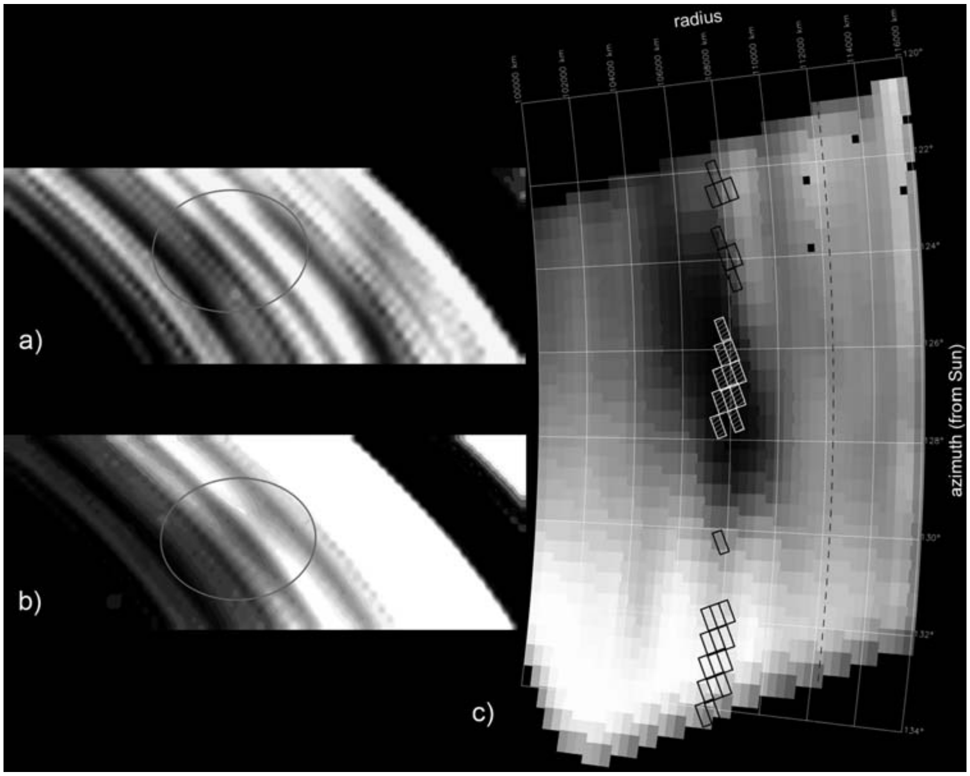

Figure 1. VIMS data (cube 1594203306) used in the analysis. (a) reflectance image from VIMS-V (λ = 0.52 μm). (b) reflectance image from VIMS-IR (λ = 2.23 μm). The faint spoke, marked by a circle, overlies the fine ring structure in both contrast-enhanced images. (c) The spoke is emphasized in this polar-projected image (λ = 2.23 μm), after azimuthal normalization of the ringlets' reflectance profiles. The actual footprints of the data selected for the spectral analysis are indicated by the boxes, white line-filled for the spoke pixels and empty black for the reference pixels. The dashed line denotes the synchronous radius in the System III reference frame.

the reflectance values, likely to be a residual of the flat field correction.

4. Spectrum of the Spoke

[5] VIMS spectra averaged inside and outside the spoke are shown in Figure 2, whose footprints are shown in Figure 1c. The two spectra appear very similar in their general shape, dominated by the water ice absorption bands (broad bands at 1.5, 2.0, 3.0 μm and shallow bands at 1.05 and 1.25 μm). The most evident change in the ice features is in the 2.0 μm band, whose depth seems to be slightly smaller in the spoke's spectrum. On the contrary, the Fresnel peak at 3.1 μm and the 4 μm region seem to be totally unaffected by the presence of the spoke. The continuum level inside the spoke appears lower than the reference spectrum everywhere shortward of about 3 μm. As pointed out by *McGhee et al.* [2005], the spectral contrast $C = 1\text{-}r_{spk}/r_{ring}$ is a meaningful quantity to measure the effect of the spoke on the ring reflectance, since it equals the spoke's optical thickness if it is optically thin. This is true however only in a non-scattering approximation of the radiative transfer inside the spoke. By its definition, C is a positive quantity for a dark spoke. The average spectral contrast of the spoke under study is reported in Figure 3. Only the 0.35–2.75 μm portion of the spectrum is shown because of very high noise longward of the 3 μm band, due to the extremely high absorption of water ice there.

[6] Several features can be noted in the contrast spectrum:

[7] 1. The spoke contrast in the NIR spectral range 1–3 μm is high, of the same order than in the VIS. As will be discussed below, this was not expected on the basis of previous observations, limited to the VIS range.

[8] 2. Shallow decreases of contrast are associated with the 1.5 μm and 2.0 μm water ice bands, suggesting smaller band depths in the spoke. The same conjecture is also suggested by the decrease of contrast in the shoulder of the 3 μm band (between 2.50 and 2.75 μm).

[9] 3. The contrast spectrum rapidly increases from 0.35 to 0.60 μm.

[10] Qualitatively, the fact that the spoke is clearly observable only shortward of about 3 μm suggests that it can only carry few particles greater than this size. Also the weak dimming of the water ice bands in the spoke hints that its particles are smaller than the B ring ones. On the other hand, sub-micron sized particles should not be able to extinct radiation so efficiently longward of $\approx$1 μm, and some contribution from larger particles are likely needed to form a spoke that is optically thick in the NIR. In order to quantify these conjectures, we need to fit the measured contrast with a synthetic spectrum derived from a radiative transfer model. We assume the spoke as a thin sheet of pure water ice particles, overlying an optically unperturbed ring. The latter hypothesis is needed in order to work directly on the spoke contrast spectrum avoiding fitting the single

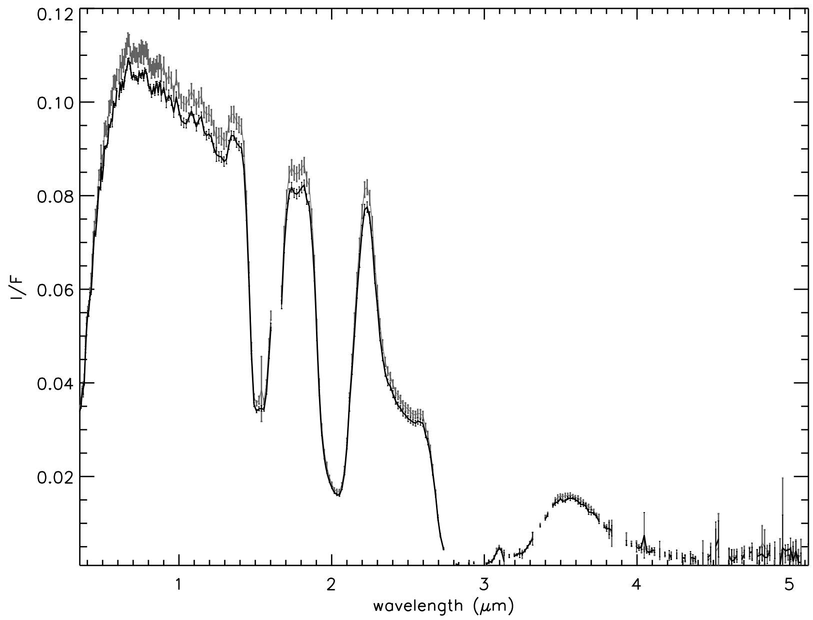

Figure 2. Full-range average VIMS spectra of spoke (black line) and ring (gray line). Error bars represent the 1-σ noise level. Bad data points have been removed.

reflectance spectra. Grains are assumed spherical in shape, with the refraction index typical of low-temperature water ice (obtained by mixing the optical constants from [*Bertie et al.*, 1969; *Toon et al.*, 1994; *Warren*, 1984; *Grundy and Schmitt*, 1998], and uniformly spatially distributed inside the spoke. The main effect of the spoke on the radiative transfer is an extinction of the radiation beam reflected by the B ring itself. This would produce a spectral contrast of the form $1 - \exp(-\tau')$ where $\tau' = \tau(\mu^{-1} + \mu_0^{-1})$ is the spoke optical thickness in the given geometry, μ_0 and μ being the cosines of the incidence and emission angles respectively. If we limit our analysis to the VIS spectral range, this term is able to fit quite well the measured contrast. The resulting grain sizes (narrowly distributed with a modal radius of about 0.65 μm with a column density of about $(60 \pm 5)10^3\mathrm{cm}^{-2}$) agree quite well with those reported by *McGhee et al.* [2005] or previously by *Doyle and Grün* [1990] using HST and Voyager data respectively. However, radiative transfer models based on such small particles fail completely in simulating the IR part of the spectrum. The high level of

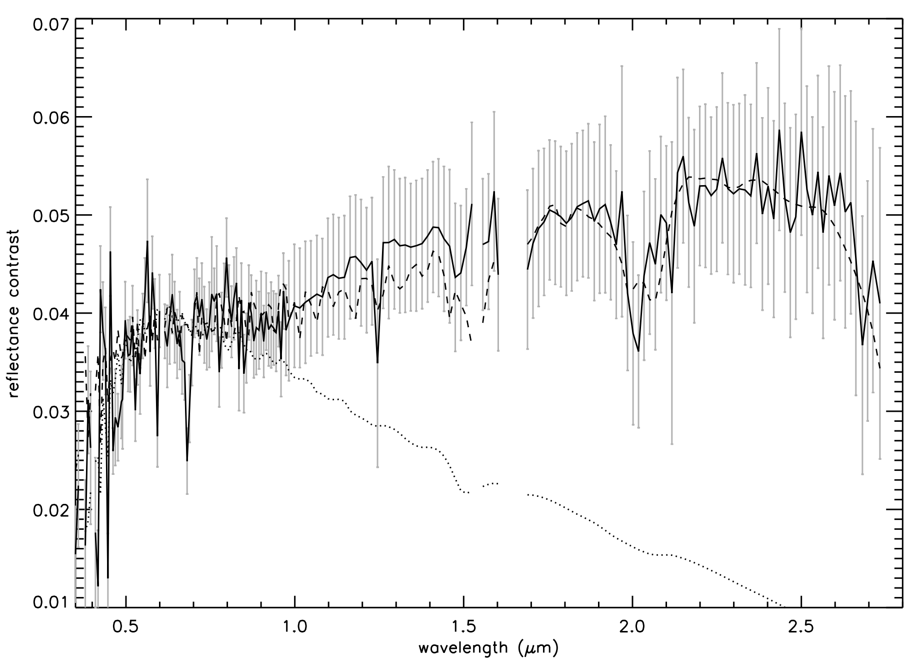

Figure 3. The solid curve represents the spectral contrast of the spoke, with 1-σ error bars. The dashed line is the best fit to the 0.35–2.75 μm range, while the dotted line is the fit to the VIS portion only.

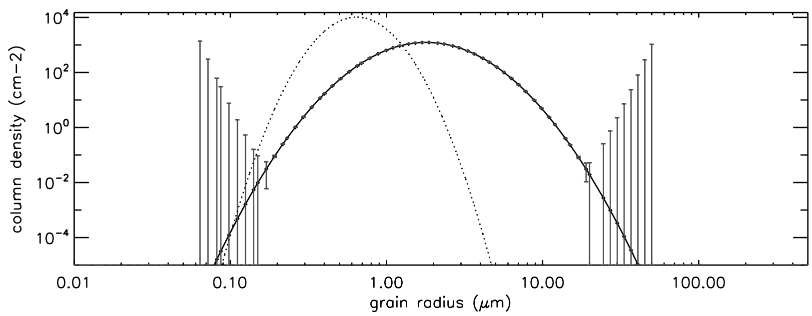

Figure 4. The solid line represents the grain size distribution associated with the 0.35–2.75 μm fit (dashed curve in Figure 3), while the dotted line refers to the VIS portion only (dotted curve in Figure 3). Formal errors due to the model sensitivity are shown as error bars.

the IR contrast in the VIMS images can be explained only if larger grains populate the spoke. Furthermore, the extinction term alone is not able to reproduce the shape of the full VIMS spectrum. We obtain better results by including the radiation scattered by the spoke's particles, with a model of the form:

$$C = 1 - e^{-\tau'} + \frac{D_1}{r_{ring}} + \frac{D_2}{r_{ring}} \quad (1)$$

where D_1 and D_2 are the once- and twice- scattered term respectively:

$$D_1 = \frac{\mu_0}{4(\mu + \mu_0)}\omega_0 p_\alpha \left(1 - e^{-\tau'}\right)$$

$$D_2 = \frac{n^2\sigma_{sca}^2}{16}\int\int \frac{p(\mu_0, \mu')p(\mu'', \mu)}{\mu'} d\mu' d\mu''$$

[11] Here ω_0 and p_α are, respectively, the single scattering albedo and phase function of the spoke particles. The scattering terms are essential in reproducing the spectral slopes and the ice band depths. The scattering in the spoke of the radiation reflected by the ring is not taken into account since, although expected to be of the same order of D_2, its evaluation requires assumptions about the B ring microphysics. Best fitting the spectral contrast in the full 0.35–2.75 μm range (Figure 3) gives a population of water ice grains with a size distribution much wider than previously thought (Figure 4). The modal radius is between 1.8 and 1.9 μm with a total column density of 14600 ± 6500 cm^{-2}. The corresponding effective quantities are r_{eff} = 3.47 μm and v_{eff} = 0.3. A model sensitivity analysis shows the distribution to be reliable between radii of 0.25 and 14 μm. The number density of spoke's grains can be calculated after making assumptions regarding the spoke vertical extent. We obtain values of $10^{-1} \div 10^{-2} cm^{-3}$ for a spoke 1 km thick, although all the retrieved density values are quite model-dependent.

5. Discussion and Conclusion

[12] The spoke observations collected in the last two decades made widely accepted the idea that they are composed of very small ice particles, lifted up from the ring boulders' surface by electrostatic forces [*Goertz and Morfill*, 1983]. Our preliminary results show that pure water ice is sufficient to explain the spoke infrared spectrum. In fact, the main feature in the spectra of the Saturn's rings related to the presence of constituents other than water ice is the blue spectral slope (0.35–0.6 μm), and its changing inside the spoke is fully reproducible by a single-constituent model. Furthermore, testing several values of refractive index between about 1.15 and 1.5, we found that the visible contrast spectrum is best fitted with values very close to that of water ice (≈1.3). Constraints on the size of the spokes' grains have been inferred by many authors from their dynamical and physical properties. For example, the phase behavior of the spokes' reflectance, brighter than the ring at high phase angles, darker at low phase angles, implies radiative scattering properties typical of small particles [*Smith et al.*, 1982]. Deviations from keplerian velocities have been used to establish lower limits of grain sizes of the order of 0.1 μm [*Thomsen et al.*, 1982], a value also suggested in early spoke formation models [*Goertz and Morfill*, 1983]. However, grains stability criteria against electrostatic and centrifugal disruption suggest the grains radii to be inside the range of 0.5–3 μm [*Thomsen et al.*, 1982; *Meyer-Vernet*, 1984], and subsequent data analyses agreed with this lower limit: Voyager photometry yielded an effective value of 0.44 ± 0.3 μm [*Doyle and Grün*, 1990], using a gamma grain size distribution with r_{eff} = 0.6 ± 0.2 μm and effective variance v_{eff} 0.09, and HST data analysis resulted in a modal radius of 0.42 ± 0.07 μm [*McGhee et al.*, 2005], r_{eff} = 0.57 ± 0.05, v_{eff} = 0.09 ± 0.03. In both cases the inferred widths of the size distributions had to be quite narrow in order to explain the data in the visible range. The VIS portion of the VIMS spectrum is not far from these results. The modal radius of 0.65 μm that we obtain in this case is even nearer to the theoretical expectation by *Goertz* [1984], predicting a peak of the size distribution around 0.6 μm, based on a meteor bombardment plasma model. However, infrared observations of spokes were not available until now, and the visibility of spokes at near-infrared wavelengths was not predictable on the basis of previous knowledge. Just the fact that spokes are observable at the VIMS infrared wavelengths with a reflectance contrast of the same order as the visible one indicates that particles of 1 μm radius or greater must substantially contribute to the spoke, at least as numerous as sub-micron ones. Our preliminary analysis of a spoke spectrum from 0.35 to 2.75 μm results in a pick radius of about 1.9 μm, with a size distribution more dispersed than previously thought (log-normal with r_{eff} = 3.5 μm, v_{eff} = 0.3). The contribution

of sub-micron particles is still relevant, but it is no more the most important, neither as number density nor, of course, as mass distribution. If 90% of particles have a radius smaller than 3.3 μm, 90% of the spoke mass is carried by particles with radii greater than about 2 μm, near the centrifugal disruption radius. A greater size of spokes' grains may have wide implications for the physical modeling of spokes. In particular the grains charging process should be strong enough to be effective on grains more massive than previously thought by 50–100 times. This new measurement should increase the lower limits of the total energy supplied to the rings in the spoke formation by at least one order of magnitude. Moreover, as pointed out by several authors, the forces governing the spokes' evolution are expected to produce significant size selection effects. Depending on the q/m ratio, electrostatic levitation is less efficient for larger grains, and may produce a vertical stratification inside the spoke affecting in turn the overall radiative transport. These effects are not taken into account in our model, and the retrieved wider size distribution may reflect a non uniform mixing of the grains with different radii. An increased spread of sizes, if confirmed, should also be taken into account in estimating the dynamical evolution of spokes, since larger grains are likely to follow different trajectories to the smaller ones, and to survive for shorter times before falling back. Finally, it is worth noting that this analysis only refers to the densest part of a single spoke. A more complete survey of the spokes observed by VIMS is needed in order to get more robust and statistically meaningful conclusions. The eventual detection of spectral variations inside a single spoke is also under investigation and will be very useful in order to retrieve both spatial and temporal variations of the spoke grains' size distribution.

[13] **Acknowledgments.** This work was supported by ASI, Agenzia Spaziale Italiana.

References

Acton, C. H. (1996), Ancillary Data Services of NASA's Navigation and Ancillary Information Facility, *Planet. Space Sci.*, *23*, 65–70.

Bertie, J. E., H. J. Labbè, and E. Whalley (1969), Absorptivity of ice I in the range 4000–30 cm^{-1}, *J. Chem. Phys.*, *50*(10), 4501.

Brown, R. H., et al. (2004), The Cassini visual and infrared mapping spectrometer (VIMS) investigation, *Space Sci. Rev.*, *115*(1–4), 111–168.

Doyle, L. R., and E. Grün (1990), Radiative transfer modeling constraints on the size of the spoke particles in Saturn's rings, *Icarus*, *85*, 168–190.

Farmer, A. J., and P. Goldreich (2005), Spoke formation under moving plasma clouds, *Icarus*, *179*, 535–538.

Goertz, C. K. (1984), Formation of Saturn's spokes, *Adv. Space Res.*, *4*(9), 137–141.

Goertz, C. K., and G. Morfill (1983), A model for the formation of spokes in Saturn's ring, *Icarus*, *53*, 219–229.

Grundy, W. M., and B. Schmitt (1998), The temperature-dependent near-infrared absorption spectrum of hexagonal H_2O ice, *J. Geophys. Res.*, *103*(E11), 25,809–25,822.

Jones, G. H., et al. (2006), Formation of Saturn's ring spokes by lightning-induced electron beams, *Geophys. Res. Lett.*, *33*, L21202, doi:10.1029/2006GL028146.

McCord, T. B., et al. (2004), Cassini VIMS observations of the Galilean satellites including the VIMS calibration procedure, *Icarus*, *172*, 104–126.

McGhee, C. A., R. G. French, L. Dones, J. N. Cuzzi, H. J. Salo, and R. Danos (2005), HST observations of spokes in Saturn's B ring, *Icarus*, *173*, 508–521.

Meyer-Vernet, N. (1984), Some constraints on particles in Saturn's Spokes, *Icarus*, *57*, 422–431.

Mitchell, C. J., M. Horànyi, O. Havnes, and C. C. Porco (2006), Saturn's spokes: Lost and found, *Science*, *311*, 1587–1589.

Morfill, G. E., and H. M. Thomas (2005), Spoke formation under moving plasma clouds—The Goertz-Morfill model revisited, *Icarus*, *179*, 539–542.

Smith, B. A., et al. (1982), A new look at the Saturn system: The Voyager 2 images, *Science*, *215*, 504–537.

Thomsen, M. F., C. K. Goertz, T. G. Northrop, and J. R. Hill (1982), On the nature of particles in Saturn's spokes, *Geophys. Res. Lett.*, *9*(4), 423–426.

Toon, O. B., M. A. Tolbert, B. G. Koehler, A. M. Middlebrook, and J. Jordan (1994), Infrared optical constants of H_2O ice, amorphous nitric acid solutions, and nitric acid hydrates, *Geophys. Res. Lett.*, *99*(D12), 25,631–25,654.

Warren, S. G. (1984), Optical constants of ice from the ultraviolet to the microwave, *Appl. Opt.*, *23*(8), 1206–1225.

F. Altieri, G. Bellucci, F. G. Carrozzo, E. D'Aversa, and F. Tosi, Istituto di Fisica dello Spazio Interplanetario, INAF, Via Fosso del Cavaliere, 100, I-00133 Rome, Italy. (emiliano.daversa@ifsi-roma.inaf.it)

R. H. Brown, Lunar and Planetary Laboratory, University of Arizona, Tucson, AZ 85721, USA.

G. Filacchione, Istituto di Fisica Spaziale e Fisica Cosmica, INAF, Via del Fosso del Cavaliere 100, I-00133 Rome, Italy.

M. M. Hedman and P. D. Nicholson, Astronomy Department, Cornell University, Ithaca, NY 14853, USA.

M. R. Showalter, SETI Institute, 515 N. Whisman Rd., Mountain View, CA 94043, USA.